GMR
The Original

ANTI-INFLAMMATORY POTENTIAL OF STARCH/PVA ELECTROSPUN NANOSCAFFOLDS EMBEDDED WITH ULTRASONIC-ASSISTED, BIOGENIC SYNTHESIZED CUO NANOPARTICLES FROM *TURBINARIA CONOIDES* (MARINE MACROALGAE) EXTRACT

Pooja Shree[1], Bhurani Ritu N[2], Sangevi Raam A[3], Anguchamy Veeruraj[4], Kaliyamoorthy Dass[5*]

[1]Saveetha Medical College & Hospital (SMCH), Saveetha Institute of Medical and Technical Sciences (SIMATS), Thandalam, Chennai, Tamil Nadu 602105, India. poojashree0513@gmail.com
[2]Postgraduate, Department of ENT, Saveetha Medical College and Hospital, Saveetha Institute of Medical And Technical Sciences (SIMATS), Thandalam, Chennai-602105, Tamil Nadu, India. Email: ritunagarajan@gmail.com; ORCID: https://orcid.org/0009-0009-9620-1088.
[3]Senior Resident, Department of Paediatrics, Saveetha Medical College and Hospital, Saveetha Institute of Medical And Technical Sciences (SIMATS), Thandalam, Chennai-602105, Tamil Nadu, India. Email: sangeviraam@gmail.com; ORCID: https://orcid.org/0009-0001-3219-0764.
[4]Saveetha Institute of Basic Medical Sciences (SIBMS), Saveetha Medical College and Hospital, Saveetha Institute of Medical and Technical Sciences (SIMATS), Saveetha University, Chennai, 602 105, Tamil Nadu, India. Email: anguveeruraj@gmail.com
Orcid ID : https://orcid.org/0000-0001-7456-6507
[5*]Natural Product and Vector Control Research Lab, Department of Pharmacology, Saveetha Medical College and Hospital, Saveetha Institute of Medical And Technical Sciences (SIMATS), Thandalam, Chennai-602105, Tamil Nadu, India. Email: dass.smc@saveetha.com; kdassrsgc1987@gmail.com, Orcid ID: https://orcid.org/0000-0002-4564-3275

ABSTRACT

This study explores the anti-inflammatory potential of starch/polyvinyl alcohol (PVA) electrospun nanoscaffolds embedded with biogenic copper oxide nanoparticles (CuO NPs) synthesized using Turbinaria conoides seaweed extract via an ultrasonic-assisted method. UV-Visible spectroscopy confirmed the formation of CuO NPs through a distinct surface plasmon resonance (SPR) peak at 270–300 nm, while Fourier Transform Infrared Spectroscopy (FTIR) analysis revealed stabilizing phytochemicals and successful integration into the polymer matrix. X-ray Diffraction (XRD) confirmed the monoclinic crystalline structure of CuO NPs, and Scanning Electron Microscopy (SEM) demonstrated uniform nanofiber morphology with well-dispersed nanoparticles. Thermogravimetric Analysis (TGA) indicated enhanced thermal stability in CuO-loaded scaffolds, while zeta potential analysis suggested moderate colloidal stability. Anti-inflammatory assays revealed concentration-dependent inhibition of protein denaturation and xanthine oxidase activity. At 100 µg/mL, the nanoscaffolds exhibited superior inhibition (78.25–79.86%) compared to standalone CuO NPs (69.86–71.25%) and algal extract (63.86–64.25%), highlighting synergistic effects from the nanocomposite structure. These findings underscore the potential of starch/PVA/CuO-NPs nanoscaffolds as advanced anti-inflammatory biomaterials, offering improved efficacy and stability for biomedical applications.

KEYWORDS: Turbinaria conoides, Green synthesis, CuO nanoparticles, Starch/PVA/CuO-NPs nanoscaffolds, Anti-inflammatory activity.

1. INTRODUCTION

Chronic inflammation is a key pathological mechanism implicated in the onset and progression of a wide range of degenerative diseases, including arthritis, cardiovascular disorders, neurodegenerative conditions, and certain cancers [1]. The prolonged activation of the inflammatory cascade leads to the excessive production of reactive oxygen species (ROS), pro-inflammatory cytokines, and degradative enzymes, which collectively cause tissue damage and functional impairment [2]. Conventional anti-inflammatory medications such as non-steroidal anti-inflammatory drugs (NSAIDs) and corticosteroids, though effective, are often associated with adverse side effects including gastrointestinal disturbances, renal toxicity, and increased cardiovascular risks [3]. As a result, there has been a growing scientific interest in the development of alternative, biocompatible, and cost-effective therapeutic platforms that can mitigate inflammation with minimal side effects [4].

In recent years, biomaterials-based approaches, particularly those involving electrospun nanofibrous scaffolds, have gained significant attention in biomedical research due to their structural resemblance to the natural extracellular matrix (ECM), high surface-to-volume ratio, and capacity to serve as drug delivery vehicles or tissue engineering templates [5]. Electrospinning is a versatile and scalable technique for fabricating ultrafine polymeric fibers with customizable physicochemical properties [6]. Among various polymer combinations, starch and polyvinyl alcohol (PVA) stand out due to their excellent biocompatibility, biodegradability, and mechanical flexibility [7]. Starch, a natural polysaccharide, offers innate hydrophilicity and structural support, while PVA enhances fiber integrity and processing efficiency during

electrospinning [8]. However, the therapeutic efficacy of polymeric nanofibers can be significantly enhanced by the incorporation of functional nanoparticles, especially those with bioactive and anti-inflammatory properties [9].

Copper oxide nanoparticles (CuO NPs) are among the most promising inorganic nanomaterials owing to their broad-spectrum biological activities, including antimicrobial, antioxidant, and anti-inflammatory effects [10]. CuO NPs have demonstrated the ability to modulate inflammatory signaling pathways, reduce oxidative stress, and inhibit key inflammatory enzymes such as cyclooxygenase and xanthine oxidase [11]. Despite their potential, the conventional synthesis of CuO NPs often involves the use of toxic chemicals, high temperatures, and energy-intensive procedures that raise environmental and safety concerns [12]. To overcome these challenges, eco-friendly, biogenic synthesis strategies employing plant or algal extracts have emerged as sustainable alternatives [13]. These biosynthetic routes utilize phytochemicals—such as polyphenols, flavonoids, and alkaloids—as reducing and capping agents, enabling the green fabrication of nanoparticles under mild conditions [14].

Marine macroalgae represent an underexplored yet highly promising resource for nanoparticle biosynthesis due to their diverse metabolite profiles and high abundance in coastal ecosystems [15]. Turbinaria conoides, a brown macroalga found abundantly along the southeastern coast of India, is rich in polysaccharides, terpenoids, and phenolic compounds with known pharmacological activities [16]. Previous studies have highlighted its potential in wound healing, antibacterial, and antioxidant applications [17]. However, its role in nanoparticle-mediated anti-inflammatory platforms remains inadequately investigated. The current study harnesses the phytochemical richness of Turbinaria conoides extract, obtained through an ultrasonic-assisted extraction process, to synthesize CuO NPs via a green synthesis route [18].

Ultrasonic-assisted extraction offers significant advantages over conventional methods by enhancing cell wall disruption, promoting the release of intracellular bioactives, and preserving thermolabile constituents [19]. The application of ultrasonication also aligns with green chemistry principles, ensuring higher extraction efficiency and lower solvent usage [20]. The phytochemical-laden algal extract not only facilitates the reduction of copper ions but also acts as a stabilizing agent, yielding CuO NPs with controlled morphology and surface properties [21]. These biosynthesized nanoparticles, when embedded into starch/PVA-based nanofibers, create a novel composite scaffold with multifunctional attributes [22]. The integration of CuO NPs into the polymeric matrix was achieved using the electrospinning technique, ensuring uniform dispersion and retention of nanoparticle activity within the scaffold [23]. The resulting starch/PVA/CuO nanofibrous scaffolds are hypothesized to exhibit synergistic anti-inflammatory effects, driven by the combinatorial benefits of the biocompatible polymer blend and the bioactive nanoparticles [24]. The physicochemical properties of the scaffolds, including morphology, thermal stability, crystallinity, and functional group interactions, were comprehensively characterized using UV–Vis spectroscopy, Fourier Transform Infrared Spectroscopy (FTIR), X-ray Diffraction (XRD), Scanning Electron Microscopy (SEM), and Thermogravimetric Analysis (TGA) analyses [25]. Additionally, particle size and zeta potential measurements were performed to assess nanoparticle stability and dispersion quality [26].

To evaluate the biological efficacy of the developed scaffolds, two well-established in vitro anti-inflammatory assays were employed: the protein denaturation inhibition assay and the xanthine oxidase inhibition assay [27]. Protein denaturation is a key marker of inflammatory response, often leading to antigen formation and tissue damage [28]. The ability of the scaffold to inhibit this process suggests its therapeutic potential [29]. Similarly, xanthine oxidase plays a central role in ROS generation during inflammation [30]. Inhibiting this enzyme indicates the scaffold's capacity to modulate oxidative pathways, contributing to overall anti-inflammatory activity [31].

This study, therefore, presents a sustainable and biologically potent nanoplatform by integrating marine-derived CuO NPs into starch/PVA electrospun scaffolds. The novelty lies in the use of Turbinaria conoides extract for green synthesis, the application of ultrasonic extraction for efficient metabolite recovery [32], and the incorporation of the nanoparticles into a biopolymeric matrix with potential biomedical applications [33]. The outcomes are expected to pave the way for the development of advanced wound dressings, tissue engineering scaffolds, or localized drug delivery systems targeting inflammatory disorders. Through this integrated approach, the research not only addresses the need for safer anti-inflammatory alternatives but also contributes to the growing field of green nanotechnology and marine biomaterial utilization.

2. MATERIALS AND METHODS

2.1. Chemicals and reagents

This study utilized Turbinaria conoides, a brown macroalga indigenous to the coastal waters near Rameswaram, Tamil Nadu, India, for the sustainable synthesis of CuO NPs. Analytical-grade copper (II) sulfate pentahydrate was used as the precursor salt. PVA with an average molecular weight of approximately 115,000 g/mol and starch were incorporated to fabricate nanofibrous scaffolds via electrospinning, using the HOLMARC HO-NFES-040 electrospinning apparatus. All chemical substances, including solvents and other reagents, were of analytical grade and obtained from Merck and Sigma-Aldrich to maintain consistency and reproducibility. The synthesized products were subjected to comprehensive physicochemical characterization and evaluated for anti-inflammatory activity using standardized bioassays.

2.2. Collection and preparation of algal biomass

Live thalli of Turbinaria conoides were hand-collected from the intertidal belt along the Rameswaram coast. Samples were promptly transported in ice-chilled containers to the laboratory. Surface debris, including epiphytes and sand, was eliminated by thoroughly washing the biomass under running tap water, followed by successive rinsing with distilled water to remove residual salts. About 100 grams of clean algae were chopped into small segments and air-dried at ambient temperature for 14 days. After complete drying, the algal biomass was ground into a uniform powder and stored in sealed containers for extraction and nanoparticle synthesis processes.

2.3. Ultrasonic extraction of phytoconstituents

For extraction of bioactive molecules, 2 grams of powdered algal material were suspended in 50 mL of Milli-Q water in a 100 mL borosilicate beaker. The suspension was subjected to ultrasonication using a LABQUEST ultrasonic cleaner (Borosil, Serial No. 941032329018) at 60°C for 45 minutes to enhance cell wall disruption and metabolite diffusion. The mixture was filtered using sterile Whatman No. 1 filter paper to remove insoluble residues. The clear filtrate was stored at 10°C for subsequent experimental use. A portion was lyophilized using a freeze-dryer to obtain a stable powder form of the extract for nanoparticle production [34, 35].

2.4. Eco-friendly synthesis of CuO NPs

To biosynthesize CuO NPs, 50 mL of 0.1 M copper sulfate solution was mixed with 10 mL of the aqueous algal extract (equivalent to 10 mg dry weight) in a 5:1 volume ratio. The mixture was stirred at 650 rpm and maintained at 60°C for 2 hours on a temperature-controlled magnetic stirrer. A visible color transition from deep blue to bluish-green indicated the successful bioreduction of copper ions, mediated by phytochemicals from the algal extract. Post-synthesis, the resulting nanoparticles were washed thrice using double-distilled water to eliminate unreacted materials and lyophilized for 48 hours to yield a dry nanoparticle powder for further study [36].

2.5. Fabrication of starch/PVA/CuO NP nanofiber scaffolds

For scaffold preparation, a 15% (w/w) aqueous solution of PVA was made by dissolving the polymer in Milli-Q water under mild heating (50°C) with continuous stirring. Upon complete dissolution, 100 mg of starch and the synthesized CuO NPs were incorporated into the solution. The mixture was further stirred at 50°C for 2.5 hours to ensure uniform dispersion. The prepared blend was loaded into a syringe fitted with a 0.84 mm stainless steel needle and subjected to electrospinning using a HOLMARC HO-NFES-040 setup. Electrospinning was conducted at ambient temperature with optimized settings: voltage of 11.5 kV, tip-to-collector distance of 12.3 cm, and flow rate of 0.4 mL/h. The process was carried out for 6 to 8 hours to obtain uniform nanofibrous scaffolds, which were then collected and stored in desiccators for characterization [37-39].

2.6. Physicochemical characterization

2.6.1. UV–visible spectroscopy

The optical profiles of the algal extract, CuO NPs, and nanocomposite scaffolds were analyzed using a VIS SPEC V-730 UV–Vis spectrophotometer. Absorbance readings were taken across a wavelength range of 200 to 800 nm, using deionized water as a blank. The presence of distinct absorption peaks, particularly between 270 and 300 nm, indicated successful nanoparticle formation and their integration into the scaffold matrix [40].

2.6.2. FTIR spectroscopy analysis

To identify functional groups and molecular interactions, FTIR analysis was performed using a PerkinElmer Spectrum Two spectrometer in ATR mode. Samples were scanned within the spectral range of 4000–400 cm^{-1} at a resolution of 4 cm^{-1}, with 64 scans per sample. Characteristic peaks corresponding to hydroxyl, carbonyl, amide, and metal–oxygen groups validated the presence of bioactive components and successful nanoparticle incorporation [41].

2.6.3. XRD analysis

The crystallinity and phase identification of CuO NPs and their dispersion in the scaffolds were analyzed using a Bruker D8 Advance X-ray diffractometer equipped with CuKα radiation (λ = 1.5406 Å). Measurements were recorded from 5° to 90° 2θ with a step size of 0.029649° at 40 kV and 40 mA. Sharp diffraction peaks corresponding to the monoclinic CuO phase confirmed the crystalline structure, while broadened peaks in composite scaffolds suggested effective nanoparticle embedding [42].

2.6.4. SEM analysis

Morphological evaluation and fiber distribution were assessed using a JEOL JSM-IT800 NANO SEM. All samples were gold-coated to improve conductivity and reduce surface charging. SEM micrographs revealed a uniform fiber diameter and homogenous nanoparticle distribution across the scaffold surface, supporting successful electrospinning [43].

2.6.5. TGA

To examine thermal behavior, TGA was conducted on a PerkinElmer TGA 8000 instrument. Approximately 5 mg of sample was heated from room temperature to 550°C at a rate of 15°C/min under a nitrogen atmosphere. The resulting thermograms revealed multi-step degradation profiles, indicating moisture loss, polymer breakdown, and the influence of CuO NPs on thermal stability enhancement [44].

2.6.6. Particle size and zeta potential measurements

The size distribution and surface charge of the CuO NPs were analyzed using a Malvern Zetasizer Ultra system. Dynamic Light Scattering (DLS) was used to determine hydrodynamic diameter, while zeta potential measurements assessed colloidal stability. Nanoparticles with zeta potential values exceeding ±30 mV were considered stable and suitable for biological applications [40]. All experimental datasets related to characterization are available on the Mendeley Data platform (DOI: 10.17632/mmyv8mmkbx.2) to promote transparency and replicability [45].

2.7. Anti-inflammatory assays

2.7.1. Protein denaturation inhibition assay

The anti-inflammatory effects of the samples were tested using a modified heat-induced protein denaturation method. Each test contained 0.45 mL of 5% aqueous bovine serum albumin and 0.05 mL of the sample (algal extract, CuO NPs, composite scaffolds, or diclofenac sodium) at concentrations of 25, 50, 75, and 100 µg/mL. The pH was adjusted to 6.3 using 1 N HCl, and samples were incubated at 37°C for 20 minutes, then heated at 57°C for 3 minutes and cooled. Denaturation-induced turbidity was measured at 660 nm using a spectrophotometer [46].

2.7.2. Xanthine oxidase inhibition assay

Xanthine oxidase inhibition was assessed using a modified established protocol. Reaction mixtures included 0.3 mL of the test sample (algal extract, CuO NPs, composite scaffolds, or diclofenac sodium) at different concentrations (25, 50, 75, and 100 µg/mL), 0.5 mL of 0.15 mM xanthine solution (in phosphate buffer, pH 7.5), and 0.2 mL of xanthine oxidase enzyme (0.1 units/mL). After 15 minutes of incubation at 25°C, absorbance was measured at 295 nm. Controls without enzyme were used for comparison [47].

2.8. Statistical analysis

All data were statistically analyzed using SPSS v25.0 and GraphPad Prism v9.0. Triplicate experiments were conducted, and data are expressed as mean ± standard deviation. Statistical significance was evaluated using one-way ANOVA followed by Tukey's or Dunnett's post-hoc test ($p < 0.05$). Normality was tested via the Shapiro–Wilk method. Log transformations were applied as needed. Correlation analyses were conducted using Pearson's correlation coefficient. A 95% confidence interval was used for all statistical interpretations [48].

3. RESULTS AND DISCUSSION

3.1. UV-visible spectroscopy

The optical profiles of the Turbinaria conoides aqueous extract, synthesized CuO NPs, and CuO-integrated starch/PVA nanoscaffolds were evaluated using UV–Visible spectroscopy. Spectra were captured using a JASCO V-730 spectrophotometer across a 200–800 nm wavelength range (Figure 1). The crude extract of Turbinaria conoides demonstrated broad absorption in the lower wavelength region, typically indicating the presence of flavonoids, polyphenols, and similar phytochemicals, which characteristically absorb UV light due to their conjugated π-electron systems [49].

In comparison, the biosynthesized CuO NPs showed a sharp absorbance peak within the 270–300 nm range, attributed to surface plasmon resonance (SPR) caused by the synchronized oscillation of conduction electrons on the nanoparticle surface upon light interaction. This distinct SPR band signifies the successful conversion of Cu2+ ions into CuO NPs, mediated by the bioactive constituents in the seaweed extract [50].

For the CuO-loaded starch/PVA nanofibrous scaffolds, the UV–Vis spectra exhibited subtle shifts and peak broadening compared to those of pure CuO NPs. These alterations suggest molecular interactions—likely hydrogen bonding or van der Waals forces—between CuO NPs and the polymer chains of starch and PVA. These spectral features confirm that CuO NPs are effectively encapsulated and uniformly distributed in the scaffold matrix. Consistent readings across three replicate runs ensured data reliability, with deionized water used as the reference blank to eliminate background interference [51, 52].

3.2. FTIR Spectroscopy analysis

To identify the functional groups involved in nanoparticle stabilization and their integration with the polymer matrix, FTIR analysis was carried out on CuO NPs and CuO-loaded scaffolds [53]. Spectra were acquired using a PerkinElmer Spectrum Two FTIR spectrometer with ATR mode, scanning from 4000 to 400 cm^{-1} at 4 cm^{-1} resolution and 64 scans [54].

The FTIR spectrum of CuO NPs (Figure 2) displayed peaks at 590.53 cm^{-1} and 464.53 cm^{-1}, confirming Cu–O stretching vibrations characteristic of copper oxide. Other notable peaks included 801.66 cm^{-1} (C–H bending), 1015.22 cm^{-1} and 1065.56 cm^{-1} (C–O stretching), and 1511.28 cm^{-1} for aromatic C=C or N–H bending. A broad peak at 3166.88 cm^{-1} suggested O–H stretching, indicative of phytochemicals from the algal extract adsorbed on the nanoparticle surface.

The FTIR spectrum of the CuO-loaded starch/PVA nanoscaffold showed modified and new bands, reflecting nanoparticle incorporation. A prominent Cu–O band at 603.51 cm^{-1} reaffirmed their presence. Additional peaks at 843.42 cm^{-1} (C–H bending), 913.12 cm^{-1} (C–O–C stretching), and 1089.99 cm^{-1} (C–O stretching) confirmed polysaccharide and ether structures. Strong bands at 1425.37 cm^{-1} and 2923.53 cm^{-1} related to C–H vibrations, while 1711.84 cm^{-1} and 1732.70 cm^{-1} peaks indicated ester and PVA carbonyl groups. A broad O–H stretch at 3296.86 cm^{-1} suggested hydrogen bonding, supporting the existence of a stable polymer-nanoparticle matrix [55, 56].

3.3. XRD analysis

XRD characterization was used to determine the crystallinity and structural integration of CuO NPs within nanoscaffolds [45]. Analysis was conducted with a Bruker D8 Advance diffractometer using CuKα radiation ($\lambda = 1.5406$ Å) at 40 kV and 40 mA, scanning 2θ from 5° to 90° with a step size of 0.029649° (Figure 3) [57].

The CuO NP diffraction pattern (Figure 3) showed sharp peaks associated with a monoclinic crystal phase, consistent with JCPDS card No. 48-1548. Key reflections appeared at 15.666°, 16.451°, 17.368°, 20.181°, 24.173°, 26.071°, 28.492°, 31.764°, 32.614°, 35.035°, 38.242°, and 47.468°. The most intense peak at 26.071° corresponded to a d-spacing of 3.41519 Å and an FWHM of 0.100°, indicating small crystalline domains.
For the CuO-integrated scaffold, the XRD pattern showed semi-crystalline features. Peaks at 11.332°, 19.284°, 21.272°, 23.481°, 29.372°, 30.771°, 35.778°, 39.533°, and 47.559° were observed. The strong reflection at 29.372° (d = 3.03842 Å, FWHM = 0.170°) indicated the polymer matrix's contribution. The presence of CuO-specific peaks at 30.771° and 35.778° affirmed nanoparticle retention. Peak broadening and shifts pointed to reduced crystallite size and strain, resulting from polymer–nanoparticle interactions. The monoclinic structure remained intact, indicating that CuO's crystalline identity was preserved post-embedding [45, 58].

3.4. SEM analysis

Morphological evaluation of CuO NPs and nanoscaffolds was conducted using a JEOL JSM-IT800 NANO scanning electron microscope [59]. Samples were gold-coated before imaging to enhance conductivity [60].
SEM images of CuO NPs showed mostly spherical particles with some irregular shapes, ranging in size from 60 to 90 nm. Some agglomeration was noted, likely due to high surface energy and particle interactions. SEM images of the CuO-starch/PVA scaffolds (Figure 4) revealed a consistent fibrous structure, with fiber diameters averaging 90–110 nm. The nanofibers had a smooth morphology and interconnected porous network, beneficial for drug delivery and tissue regeneration due to enhanced cell adhesion and nutrient exchange.
CuO NPs were clearly embedded within the fibers, appearing evenly distributed and minimally aggregated, indicating successful electrospinning integration. The uniformity of nanoparticle dispersion and consistent fiber formation demonstrated that process parameters were well-optimized for producing stable, functional nanocomposite scaffolds [61].

3.5. TGA

The thermal degradation profile of CuO-incorporated nanofibers was examined using a PerkinElmer TGA 8000 analyzer. A 7.685 mg sample was heated from 30°C to 550°C at 15°C/min under nitrogen flow (Figure 5).
The thermogram revealed two major decomposition stages. The initial degradation began at 326.78°C, peaked at 381.60°C, and accounted for a 34.960% mass loss, corresponding to the breakdown of starch, PVA, and volatile compounds. The second degradation started at 438.61°C, peaking at 459.06°C, causing an additional 4.679% weight loss, attributed to residual organics and CuO-bound bioactives.
CuO NPs enhanced the scaffold's thermal resilience. Compared to neat starch/PVA composites, the CuO-based nanocomposites exhibited a delayed onset of degradation, indicating better thermal stability due to the inorganic CuO limiting polymer chain mobility. DTG plots further clarified these transitions. The low residual mass after 550°C suggested that most organics had decomposed, with CuO acting as a thermal stabilizer in the matrix [62-64].

3.6. Zeta potential and particle size analysis

DLS and zeta potential measurements were used to assess the size distribution and surface charge of CuO NPs using a Malvern Zetasizer Ultra. The hydrodynamic diameter had a dominant peak at 68.6 nm (Figure 6), aligning with SEM findings. The polydispersity index (PDI) was 0.5717, reflecting moderate particle size variability.
Zeta potential measurements showed a main surface charge of -11.39 mV, with minor peaks at -42.6 mV and -12.28 mV (Figure 7). The primary zeta value indicates limited electrostatic repulsion, suggesting potential for slight aggregation over time. However, the presence of a fraction with higher negative charge implies partial colloidal stability, although the overall stability falls below the ±30 mV threshold generally considered ideal.
The system's conductivity (0.06892 mS/cm) and count rate (3.27×10^4 kcps) supported good dispersion. However, for improved long-term dispersion in biomedical applications, surface functionalization or stabilizing agents may be necessary. These findings provide essential insights into the colloidal stability and potential biomedical utility of CuO NPs [65, 66].

3.7. Anti-inflammatory assays:

3.7.1. Protein denaturation inhibition assay

The protein denaturation inhibition assay (Figure 8) evaluated the anti-inflammatory potential of algal extract, CuO NPs, and starch/PVA/CuO-NPs nanoscaffolds by measuring their ability to prevent heat-induced denaturation of bovine serum albumin (BSA) [67]. The results demonstrated concentration-dependent inhibition across all tested samples [68].
At the lowest concentration (25 µg/mL), the algal extract exhibited 19.05–19.66% inhibition, while CuO NPs showed a higher efficacy (23.66–25.05%). The nanoscaffolds displayed the strongest inhibition (26.66–27.05%), suggesting enhanced anti-inflammatory properties due to the composite structure. As concentrations increased to 100 µg/mL, the inhibition percentages rose significantly: algal extract (63.86–64.25%), CuO NPs (69.86–71.25%), and nanoscaffolds (78.25–79.86%). Notably, the nanoscaffolds consistently outperformed both the algal extract and CuO NPs, indicating synergistic effects from the starch/PVA matrix and CuO NPs.

3.7.2. Xanthine oxidase inhibition assay

The xanthine oxidase inhibition assay (Figure 8) assessed the ability of the samples to suppress uric acid formation, a key marker of inflammation. Similar to the protein denaturation assay, all samples exhibited concentration-dependent activity [69].

At 25 µg/mL, the algal extract inhibited xanthine oxidase by 19.05–19.66%, while CuO NPs showed 23.66–25.05% inhibition. The nanoscaffolds again demonstrated superior performance (26.66–27.05%). At higher concentrations (100 µg/mL), the inhibition rates increased substantially: algal extract (63.86–64.25%), CuO NPs (69.86–71.25%), and nanoscaffolds (78.25–79.86%). The nanoscaffolds' enhanced efficacy may stem from improved stability and controlled release of CuO NPs within the polymeric matrix.

Both assays confirmed that the starch/PVA/CuO-NPs nanoscaffolds exhibited the highest anti-inflammatory activity, followed by CuO NPs and the algal extract. The nanoscaffolds' superior performance suggests that the combination of CuO NPs with a biocompatible polymer enhances anti-inflammatory effects, possibly due to improved bioavailability or sustained release. These findings highlight the potential of nanoscaffolds as advanced anti-inflammatory agents, outperforming individual components at equivalent concentrations. The results demonstrate significant anti-inflammatory properties for all tested samples, with nanoscaffolds emerging as the most effective, offering promising applications in biomedical and therapeutic fields.

5. CONCLUSION

The present study successfully demonstrated the synthesis and characterization of starch/PVA-based electrospun nanoscaffolds embedded with biogenically synthesized CuO NPs using Turbinaria conoides extract. Comprehensive analyses, including UV–Vis, FTIR, XRD, SEM, TGA, and zeta potential, confirmed the effective integration, stability, and uniform distribution of CuO NPs within the polymer matrix. The nanoscaffolds exhibited favorable morphological and thermal properties, essential for biomedical applications. Notably, the anti-inflammatory assays revealed significant, concentration-dependent inhibitory effects, with the nanoscaffolds outperforming both the CuO NPs and the algal extract alone. This enhanced bioactivity is attributed to the synergistic interaction between CuO NPs and the biopolymer scaffold, facilitating improved stability and sustained release. These findings underscore the potential of this green-synthesized nanocomposite as a promising anti-inflammatory biomaterial for therapeutic applications. Future investigations involving in vivo models and mechanistic studies are warranted to further validate the clinical relevance and expand the biomedical utility of these eco-friendly nanoscaffolds.

Ethical Declaration: Not applicable for this study.

Funding: Not available for this study.

Conflicts of Interest: The authors declare no conflicts of interest.

Data Availability Statement: The full dataset of physiochemical characterization associated with this work is published in Mendeley Data [Dataset] Green nanotechnology in biomaterials: characterization of starch-based scaffolds with Turbinaria conoides-synthesized copper oxide nanocomposites (DOI: 10.17632/mmyv8mmkbx.1). Disclosure: The material characterization data and figures (e.g., UV, SEM, FTIR, XRD, TGA, Zeta Potential and particle sizer) presented here were generated from a common dataset and are being reused across multiple related studies on nanomaterials. All biological analyses and conclusions are original to each manuscript.

REFERENCES

1. Leyane TS, Jere SW, Houreld NN. Oxidative stress in ageing and chronic degenerative pathologies: molecular mechanisms involved in counteracting oxidative stress and chronic inflammation. International journal of molecular sciences. 2022;23(13):7273.
2. Tu H, Li Y-L. Inflammation balance in skeletal muscle damage and repair. Frontiers in immunology. 2023;14:1133355.
3. Sohail R, Mathew M, Patel KK, Reddy SA, Haider Z, Naria M, et al. Effects of non-steroidal anti-inflammatory drugs (NSAIDs) and gastroprotective NSAIDs on the gastrointestinal tract: a narrative review. Cureus. 2023;15(4).
4. Goyal AK, Ramchandani M, Basak T. Recent advancements, challenges, and future prospects in usage of nanoformulation as theranostics in inflammatory diseases. Journal of Nanotheranostics. 2023;4(1):106-26.
5. Mamidi N, García RG, Martínez JDH, Briones CM, Martinez Ramos AM, Tamez MFL, et al. Recent advances in designing fibrous biomaterials for the domain of biomedical, clinical, and environmental applications. ACS Biomaterials Science & Engineering. 2022;8(9):3690-716.
6. Cho Y, Beak JW, Sagong M, Ahn S, Nam JS, Kim ID. Electrospinning and Nanofiber Technology: Fundamentals, Innovations, and Applications. Adv Mater. 2025:2500162.
7. Elgharbawy AS, El Demerdash A-GM, Sadik WA, Kasaby MA, Lotfy AH, Osman AI. Enhancing the Biodegradability, Water Solubility, and Thermal Properties of Polyvinyl Alcohol through Natural Polymer Blending: An Approach toward Sustainable Polymer Applications. Polymers. 2024;16(15):2141.
8. Wang Y, Khan MA, Chen K, Zhang L, Chen X. Electrospinning of natural biopolymers for innovative food applications: A review. Food and Bioprocess Technology. 2023;16(4):704-25.
9. El-Aassar M, Ibrahim OM, Al-Oanzi ZH. Biotechnological applications of polymeric nanofiber platforms loaded with diverse bioactive materials. Polymers. 2021;13(21):3734.
10. Saleem MH, Ejaz U, Vithanage M, Bolan N, Siddique KH. Synthesis, characterization, and advanced sustainable applications of copper oxide nanoparticles: a review. Clean Technologies and Environmental Policy. 2024:1-26.

11. Kunamalla R, Panagal M, Palanisamy CP. Biogenic synthesis and fabrication of starch/PVA/CuO electrospun nanoscaffolds from Sargassum ilicifolium (brown marine macroalgae) extract for anticancer activity on HT-29 and MCF-7 cancer cells. Biocatalysis and Agricultural Biotechnology. 2026; 72: 103923.
12. Pei J, Govindaraj H, Sivaramakrishnan R, Kanniappan GV, Pandurangan V, Dhayalan VK, Mironescu M, Mironescu ID, Jayaraman S, Palanisamy PC. Sustainable fabrication of biopolymer-based (starch/PVA) nanoscaffolds loaded with green-synthesized CuO nanoparticles from Sargassum wightii (marine macroalgae): Cytocompatibility and antioxidant activity. Biomaterials Advances. 2026; 182: 214660.
13. Pei J, Perumal NC, Meng P, Long Q, Palanisamy CP. Extracellular vesicle-based biosensors for Alzheimer's disease: A new frontier in precision diagnostics. Ageing Research Reviews. 2026; 113: 102904.
14. Shree P, Sivaramakrishnan R, Kanniappan GV, Pandurangan V, Jayaraman S, Dhayalan VK, Mironescu M, Mironescu ID, Palanisamy CP. Antioxidant and biocompatible CuO-starch/PVA nanoscaffolds via ultrasonic green synthesis using Turbinaria conoides (brown marine macroalgae). Medicine in Drug Discovery. 2025; 28: 100238.
15. Gong J, Lin J, Guan T, Pei J, Palanisamy CP, El-AtyFrom AMA. selenium tolerance to nanoplastic antagonism: Comprehensive characterization of L. casei SNUT1 and its extracellular vesicle–nanoselenium complex. Food Bioscience. 2025; 74: 107749.
16. Poochi SP, Sundarraj R, Raju MV, Chandrasekaran MK, Ahalliya RM, Palanisamy CP, Kanniappan GV, Kondapavuluri BK, Thiruvengadam M. Harnessing Nature: Computational and Experimental Insights Into Ipomoea obscura Metabolites for Bladder Cancer Therapy. Chemistry and Biodiversity. 2025; 0: e00909.
17. Dugganaboyana GK, Kannankumar MKG, Shivaramakrishna S, Raju MV, Chandrasekaran MK, Ahalliya RM, Panneerselvam N, Palanisamy CP, Kanniappan GV. Phytochemical insights, antioxidant activity and therapeutic potential of Cassia senna against prostate cancer in Wistar albino rats. Discover Applied Sciences. 2025; 7:1206.
18. Natarajan SR, Krishnamoorthy R, Alshuniaber MA, Gatasheh MK, Rajagopal P, Veeraraghavan VP, Palanisamy CP, Jayaraman S. KDM1A Facilitates Oncogenic Potential in Colorectal Cancer Progression Through the Activation of AXIN/GSK3β/β-Catenin Signaling Pathways: Evidence From Integrated Transcriptomics and In Vitro Studies. The Journal of Gene Medicine. 2025; 27(11): e70053.
19. Guan T, Gong J, Lin J, Palanisamy CP, Jinjin Pei J, El-Aty AMA. Machine learning-driven multimodal optimization of selenium biotransformation and flavor profiling in fermented apple–Yacon functional beverages. Innovative Food Science & Emerging Technologies. 2025; 105: 104198.
20. Natarajan SR, Krishnamoorthy R, Alshuniaber MA, Alsulami TS, Gatasheh MK, Rajagopal P, Palanisamy CP, Govindan R, Veeraraghavan VP, Jayaraman S. ABCE1 facilitates tumour progression via aerobic glycolysis and inhibits cell death in human colorectal cancer cells through the p53 signalling pathway. Scientific Reports. 2025; 15: 24674.
21. Huang Y, Guo H, Liu Y, Jin W, Palanisamy CP, Pei J, Oz F, El-Aty AMA. Effects of Natural Polysaccharides on the Gut Microbiota Related to Human Metabolic Health. Molecular Nutrition & Food Research. 2025; 69:e202400792.
22. Poornima K, Meenakshi K.C, Manikandan V.R, Shankari G, Prabhu D, Rathi M.A, Palanisamy CP, Balaji R, Gopalakrishnan V.K. Exploring the anticancer potential of Jerantinine A from Tabernaemontana coronaria against prostate, breast, and ovarian cancers: A computational approach. Journal of Complementary and Integrative Medicine, 2025 22(2): 363–372.
23. Palanisamy CP, Poompradub S, Sansanaphongpricha K, Jayaraman S, Subramani K. Faridah Sonsudin gGreen synthesis of Nigella sativa-mediated silver nanoparticles for enhanced antibacterial activity and wound healing: Mechanistic insights and biomedical applications. Environmental Nanotechnology, Monitoring & Management. 2025; 24: 101085.
24. Surendran N, Raju MV, Chandrasekaran MK, Ahalliya RM, Palanisamy CP, Chandrasekaran G, Kanniappan GV. Physicochemical characterization of starch from Maranta arundinacea L.(arrowroot) rhizomes and its inhibition of COX-2: In vivo validation. Bioactive Carbohydrates and Dietary Fibre. 2025; 33: 100465.
25. Kannappan P, Chandrasekaran MK, Raju MV, Gopalakrishnan S, Dhamodharan P, Ahalliya RM, Palanisamy CP, Raju B, Kanniappan GV. Exploring the anticancer potential of Jerantinine A from Tabernaemontana coronaria against prostate, breast, and ovarian cancers: a computational approach. Journal of Complementary and Integrative Medicine. 2025; 22(02): 363-372.
26. Pei J, Kumarasamy RV, Jayaraman S, Kanniappan GV, Long Q, Palanisamy CP. Quercetin-functionalized nanomaterials: Innovative therapeutic avenues for Alzheimer's disease management. Ageing Research Reviews. 2025; 104: 102665.
27. Jayaraman S, Prasad M, Natarajan SR, Krishnamoorthy R, Alshuniaber MA, Gatasheh MK, Veeraraghavan VP, Rajagopal P, Palanisamy CP. Molecular mechanisms underlying the effects of beta-sitosterol on TGF-β1/Nrf2/SIRT1/p53-mediated signaling in the kidney of a high-fat diet and sucrose-induced type-2 diabetic rat. Chemico-Biological Interactions. 2025; 411: 111443.
28. Huang Y, Guo H, Liu Y, Jin W, Palanisamy CP, Pei J, Oz F, El-Aty AMA. Effects of Natural Polysaccharides on the Gut Microbiota Related to Human Metabolic Health. Molecular Nutrition & Food Research. 2025; e202400792.
29. Prabhakaran P, Palanisamy CP, Shanmugam A, Damodharan P, Swaminathan H, Devaraj D, Ahalliya RM, Kanniappan GV. Isolation, structural characterization, and molecular docking studies on the bioactive compound from n-Hexane extract of Emilia sonchifolia (L.) DC against the pancreatic cancer target Aurora 2 Kinase. Journal of Complementary and Integrative Medicine. 2024; 22(1): 0290.
30. Jiang H, Kumarasamy RV, Pei J, Raju K, Kanniappan GV, Palanisamy CP. Integrating engineered nanomaterials with extracellular vesicles: Advancing targeted drug delivery and biomedical applications. Frontiers in Nanotechnology. 2024; 6: 1513683.

31. Guo H, Liu Y, Wan T, Song D, Palanisamy CP, Geng J, Pei J, Özmen S, El-Aty AMA. Toward personalized cancer management: Role of precision nutrition–diet interventions. Journal of Functional Foods. 2024; 123: 106584.
32. Natarajan SR, Krishnamoorthy R, Alshuniaber MA, Al-Anazi KM, Farah MA, Rajagopal P, Palanisamy CP, Veeraraghavan VP, Jayaraman S. Identification of FOXM1 as a novel protein biomarker and therapeutic target for colorectal cancer progression: Evidence from immune infiltration and bioinformatic analyses. International Journal of Biological Macromolecules. 282 (Part 4): 137201.
33. Rajendran MS, Jayaraman S, Khan JM, Jasmine S, Prabhakaran RK, Raju MV, Chandrasekaran MK, Ahalliya RM, Kannappan P, Palanisamy CP, Kanniappan GV. Investigating the colon toxicity and carcinogenic role of monosodium glutamate compared with Dimethylhydrazine in male Wistar rats: Exploring the link to childhood colon cancer risk. Journal of King Saud University - Science. 2024; 36(11): 103507.
34. Kumarasamy RV, Natarajan PM, Umapathy VR, Roy JR, Rab SO, Saeed M, Panagal M, Mironescu M, Srinivasan GP, Palanisamy CP. Clinical Applications and Therapeutic Potentials of Advanced Nanoparticles: A Comprehensive Review on Completed Human Clinical Trials. Frontiers in Nanotechnology. 2024; 6:1479993.
35. Jin W, Pei JJ, Roy JR, Jayaraman S, Ahalliya RM, Kanniappan GV, Mironescu M, Palanisamy CP. Comprehensive review on single-cell RNA sequencing: A new frontier in Alzheimer's disease research. Ageing Research Reviews. 2024; 274: 102454.
36. Surendran N, Chandrasekaran G, Raju MV, Chandrasekaran MK, Ahalliya RM, Palanisamy CP, Kanniappan GV, Arcot R, Alharbi NS, Thiruvengadam M. Anti-inflammatory potential of ethanolic extract of Maranta arundinacea L.: Insights from COX-2 modulation and oxidative stress analysis. South African Journal of Botany. 2026; 195: 142-151.
37. Pei J, Senthilkumar MV, Hessini K, Subramaniyam S, Sivaramakrishnan R, Kanniappan GV, Jayaraman S, Palanisamy CP. Green fabrication of starch/PVA/CuO nanoscaffolds using marine macroalgae extract for enhanced anti-inflammatory activity. Sustainable Chemistry and Pharmacy. 2026; 51: 102397.
38. Balasubramanian V, Loganathan L, Muthuswamy K, Viswanathan TM, Raju MV, Chandrasekaran MK, Ahalliya RM, Poorasamy J, Palanisamy CP, Dominic S, Kanniappan GV. Anticancer therapeutic efficacy of PEGylated β-galactosidase from Aspergillus terreus in DMBA-induced breast cancer: Toxicological, molecular and histopathological evaluation in Wistar rats. International Journal of Biological Macromolecules. 2026; 360: 151856.
39. Jayaraman S, Eswaran A, Rajagopal P, Palanisamy CP, Veerakumar P, Veeraraghavan VP, Sirasanagandla SR. Neuroendocrine-associated epigenetic factors in cellular senescence: mechanisms and therapeutic implications. Biogerontology. 2026; 27(2): 64.
40. Ponnusamy B, Rajagopal P, Palanisamy CP, Veeraraghavan VP, Jayaraman S. Mechanistic Exploration of the anticancer activity of Justicia adhatoda Plant Leaf Ethanolic Extract against Colon Cancer Cells: An in silico and in vitro Approach. Asian Pacific Journal of Cancer Prevention. 2026; 27(3): 1069-1080.
41. Pei J, Saran VS, Sivaramakrishnan R, Kanniappan GV, Pandurangan V, Jayaraman S, Dhayalan VK, Mironescu M, Mironescu ID, Palanisamy CP. Ultrasonic-assisted, Sargassum ilicifolium (brown marine macroalgae)-mediated biogenic synthesis of CuO nanoparticles incorporated in starch/PVA electrospun nanoscaffolds: In vitro safety and antioxidant efficacy assessment. Bioorganic Chemistry. 2026; 173: 109679.
42. Raj MAPA, Subramaniyam S, Kanniappan GV, Jayaraman S, Palanisamy CP. Sustainable fabrication of starch/PVA/CuO electrospun nanoscaffolds from Turbinaria ornata (marine macroalgae) extract: Physicochemical characterization and antidiabetic evaluation. Kuwait Journal of Science. 2026; 53(2): 100545.
43. Pei J, Ganesh NS, Subramaniyam S, Sivaramakrishnan R, Kanniappan GV, Jayaraman S, Palanisamy CP. Sustainable fabrication of starch/PVA/CuO electrospun nanoscaffolds from Padina tetrastromatica (Brown macroalgae) extract: Physicochemical characterization and antidiabetic assessment. Sustainable Chemistry One World. 2026; 9: 100195.
44. Sakthiraj A, Sivaramakrishnan R, Subramaniyam S, Kanniappan GV, Pandurangan V, Jayaraman S, Dhayalan VK, Mironescu M, Mironescu ID, Palanisamy CP. Chemical Physics Impact. Starch/PVA electrospun nanoscaffolds loaded with ultrasonic-assisted green-synthesis of CuO nanoparticles from marine macroalgae (Gracilaria corticata) extract: Cytotoxicity and antioxidant analysis. 2026; 12: 101018.
45. Raju M, Chandrasekaran MK, Loganathan L, Ahalliya RM, Mironescu M, Mironescu ID, Palanisamy CP, Kanniappan GV. Lipid remodeling and ferroptosis in phosphatidylcholine-mediated tumor–stroma crosstalk. Frontiers in Molecular Biosciences. 2026; 13: 1742305.
46. Pei J, Palanisamy CP, Jayaraman S, Natarajan PM, Umapathy VR, Roy JR, Panagal M, Jayaraman S. Curcumin-loaded polymeric nanomaterials as a novel therapeutic strategy for Alzheimer's disease: A comprehensive review. Ageing Research Reviews. 2024; 99: 102393.
47. Pei J, Palanisamy CP, Jayaraman S, Natarajan PM, Umapathy VR, Roy JR, Thalamati D, Ahalliya RM, Kanniappan GV*, Mironescu M. A comprehensive review on starch-based Sustainable Edible Films Loaded with Bioactive Components for Food Packaging. International Journal of Biological macromolecules. 2024; 274 (Part-1): 133332.
48. Palanisamy CP, poompradub S, Sansanaphongpricha K, Subramani K, Sonsudin F. Increased expression levels of PDGF and VEGF magnify the wound healing potential facilitated by biogenic synthesis of silver nanoparticles. Nano-Structures & Nano-Objects. 2024; 39: 101236.
49. Pei J, Palanisamy CP, Jayaraman S, Natarajan PM, Umapathy VR, Roy JR, Thalamati D, Ahalliya RM, Kanniappan GV, Mironescu M. Proteomics Profiling of Extracellular Vesicle for Identification of Potential Biomarkers in Alzheimer's Disease: A Comprehensive Review. Ageing Research Reviews. 2024; 99: 102359.
50. Xi J, Wang T, Xian P, Liu X, Du M, Yang H, Palanisamy CP, Lin W, Long Q. Proteomic insights uncover enhanced neurotherapeutic potential in conditioned mesenchymal stem cell-derived extracellular vesicles. Extracellular Vesicle. 2024; 3: 100037.

51. Pei J, Natarajan PM, Umapathy VR, Swamikannu B, Sivaraman NM, Krishnasamy L, Palanisamy CP. Advancements in the synthesis and functionalization of zinc oxide-based nanomaterials for enhanced oral cancer therapy. Molecules. 2024; 29(11): 2706.
52. Gatasheh MK, Natarajan SR, Krishnamoorthy R, Alsulami TS, Rajagopal P, Palanisamy CP, Veeraraghavan VP, Jayaraman S. Molecular analysis to identify novel potential biomarkers as drug targets in colorectal cancer therapy: an integrated bioinformatics analysis. Molecular and Cellular Oncology. 2024; 11(1): 2326699.
53. Pei J, Yan Y, Jayaraman S, Rajagopal P, Natarajan PM, Umapathy VR, Gopathy S, Roy JR, Sadagopan CS, Thalamati D, Palanisamy CP, Mironescu M. A review on advancements in the application of starch-based nanomaterials in biomedicine: Precision drug delivery and cancer therapy. International Journal of Biological Macromolecules. 2024; 130746.
54. Pei JJ, Yan Y, Palanisamy CP, Jayaraman S, Natarajan PM, Umapathy VR, Gopathy S, Roy JR, Sadagopan JC, Thalamati D, Mironescu M. Materials-based drug delivery approaches: Recent advances and future perspectives. Green Processing and Synthesis. 2024; 13: 20230094.
55. Panneerselvam S, Viswaja K, Deepa E, Prathiba S, Rebecca FS, Nivedha RP, Rajagopal P, Veeraraghavan VP, Sridevi G, Palanisamy CP, Jayaraman S. Hypoglycemic Potential of Acalypha indica in Streptozotocin-Induced Type 2 Diabetic Rats. International Journal of Drug Delivery Technology. 2026; 16(26s):1038-1047.
56. Panneerselvam S, Viswaja K, Prathiba S, Rebecca FS, Nivedha RP, Rajagopal P, Fathima SJH, Veeraraghavan VP, Sridevi G, Palanisamy CP, Jayaraman S. Acalypha Indica Attenuates Insulin Resistance in STZ-Induced Type 2 Diabetic Male Rats: Mechanistic Study. International Journal of Drug Delivery Technology. 2026; 16(26s):1027-1037.
57. Manju NE, Natarajan A, Rebecca FS, Nivedha RP, Hemalatha R, Rajagopal P, Murali R, Veeraraghavan VP, Sridevi G, Palanisamy CP, Jayaraman S. Effect of Seendhil polyherbal formulation in attenuating type-2 diabetes in STZ-induced experimental rats. International Journal of Drug Delivery Technology. 2026; 16(26s):981-989.
58. Manju NE, Natarajan A, Rebecca FS, Nivedha RP, Hemalatha R, Rajagopal P, Murali R, Veeraraghavan VP, Sridevi G, Palanisamy CP, Jayaraman S. Molecular mechanism to identify the effects of Seendhil polyherbal preparation on IRS-1/AKT/GLUT4/NRF2-KEAP-1 mediated signaling in SFZ-induced type-2 diabetic adult male rats. International Journal of Drug Delivery Technology. 2026;16(26s):972-980.
59. Palanisamy CP, Poompradub S, Sansanaphongpricha K, Jayaraman S, Subramani K, Sonsudin F. Biosynthesis of silver nanoparticles (AgNPs) using ethanolic extract of Nigella sativa (L.) seeds promotes wound healing via PDGF and VEGF signalling pathways activation. Biocatalysis and Agricultural Biotechnology. 2023; 54: 102970.
60. Palanisamy CP, Pei JJ, Phaniendra A, Venkata AAN, Jayaraman S, Veeraragahavan VP, Sridevi G, Roy JR, Janaki CS, Thalamati D, Mironescu M, Luo Q, Chai Y, Long Q. New Strategy of Neurodegenerative Disease Treatment with Extracellular Vesicles (EVs) Derived from Mesenchymal Stem Cells (MSCs). Theranostics. 2023; 13(12):4138-4165.
61. Zhang Y, Zhang M, Cheng D, Xu S, Du C, Xie L, et al. Applications of electrospun scaffolds with enlarged pores in tissue engineering. Biomaterials Science. 2022;10(6):1423-47.
62. Chandel S, Pandey P, Saini S, Sharma R, Parashar B, Yadav K. Natural Product-Loaded PCL and PLA-Based Bio-Scaffold and Their Applications. Natural Product Inspired Scaffolds: Applications in Tissue Engineering. Springer; 2024. p. 117-46.
63. Le TDH, Tuan HNA, Nguyen VT, Le AT. Hydroxyapatite− loaded starch/polyvinyl alcohol scaffold for bone regeneration application: preparation and characterization. Journal of Sol-Gel Science and Technology. 2023;107(2):441-51.
64. Ramezani M, Ripin ZM. An overview of enhancing the performance of medical implants with nanocomposites. Journal of Composites Science. 2023;7(5):199.
65. Alizadeh SR, Ebrahimzadeh MA. Characterization and anticancer activities of green synthesized CuO nanoparticles, a review. Anti-Cancer Agents in Medicinal Chemistry (Formerly Current Medicinal Chemistry-Anti-Cancer Agents). 2021;21(12):1529-43.
66. Weiss M, Fan J, Claudel M, Sonntag T, Didier P, Ronzani C, et al. Density of surface charge is a more predictive factor of the toxicity of cationic carbon nanoparticles than zeta potential. Journal of nanobiotechnology. 2021;19:1-19.
67. Kola P, Metowogo K, Manjula S, Katawa G, Elkhenany H, Mruthunjaya K, et al. Ethnopharmacological evaluation of antioxidant, anti-angiogenic, and anti-inflammatory activity of some traditional medicinal plants used for treatment of cancer in Togo/Africa. Journal of Ethnopharmacology. 2022;283:114673.
68. Mendez-Encinas MA, Valencia D, Ortega-García J, Carvajal-Millan E, Díaz-Ríos JC, Mendez-Pfeiffer P, et al. Anti-inflammatory potential of seasonal sonoran propolis extracts and some of their main constituents. Molecules. 2023;28(11):4496.
69. Al-Dulaimy WYM, Hussein AA, Mahdi MA, Kadhom M. In Vitro Inhibition of Xanthine Oxidase Purified from Arthritis Serum Patients by Nanocurcumin and Artemisinin Active Compounds. Molecules. 2023;28(13):5124.

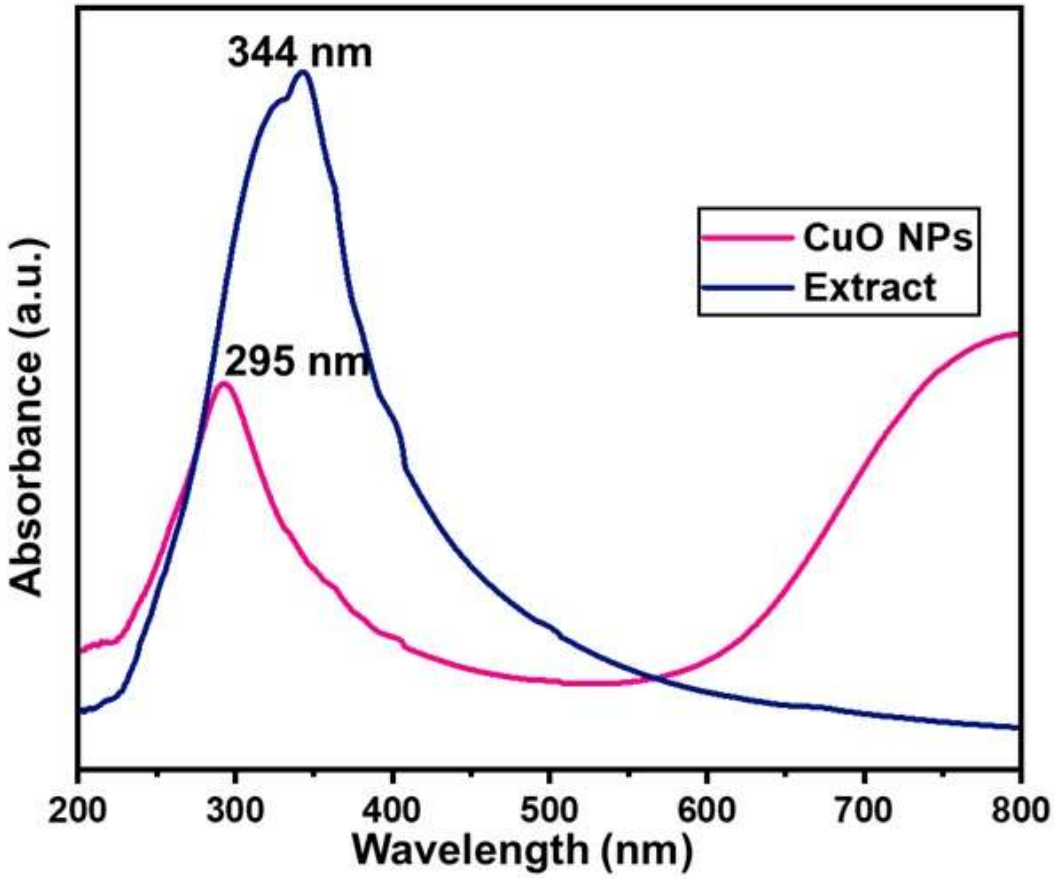

Figure 1. UV–Visible spectral profiles of algal extract and CuO NPs.

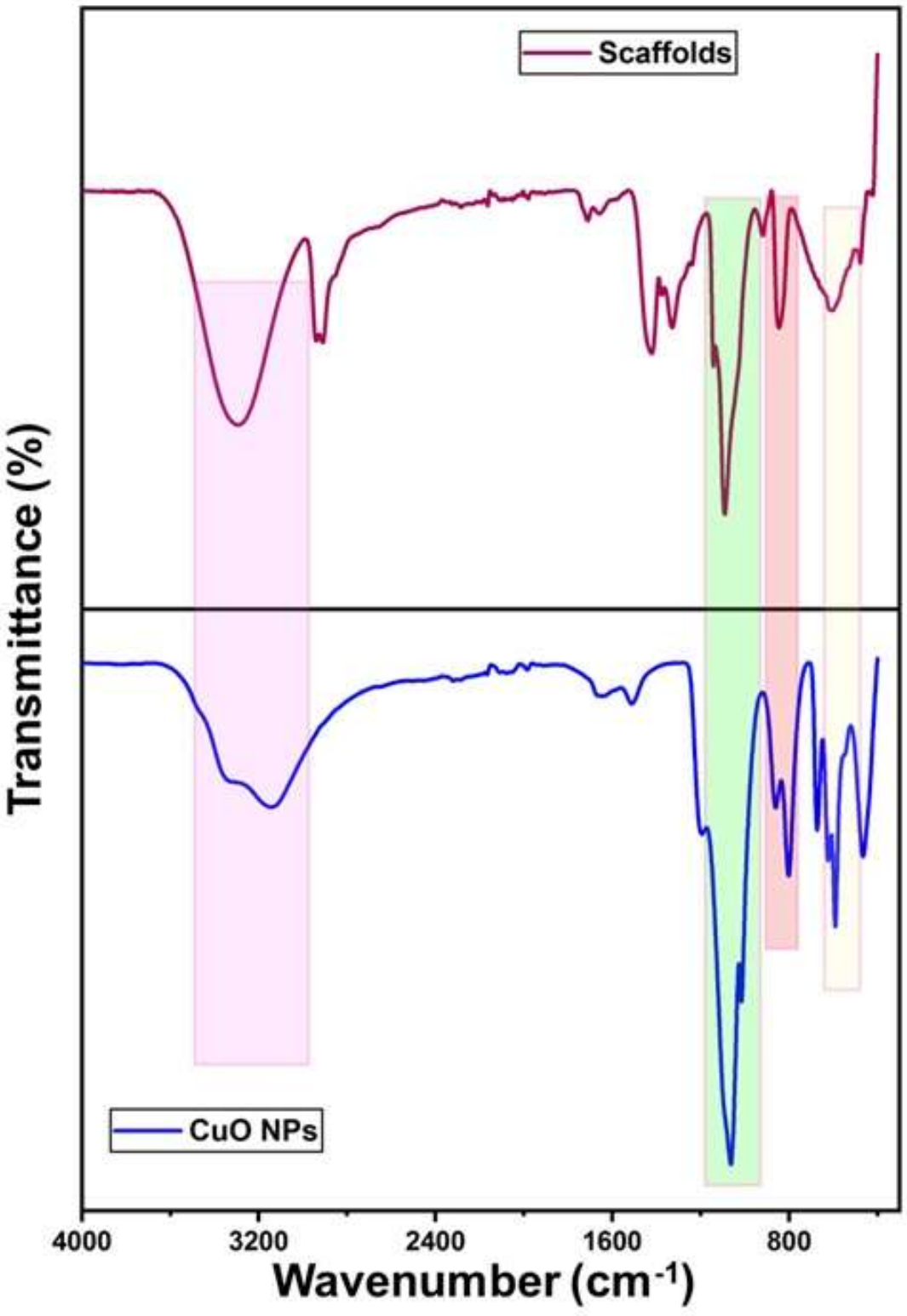

Figure 2. FTIR spectra of CuO NPs and their incorporation into nanoscaffolds.

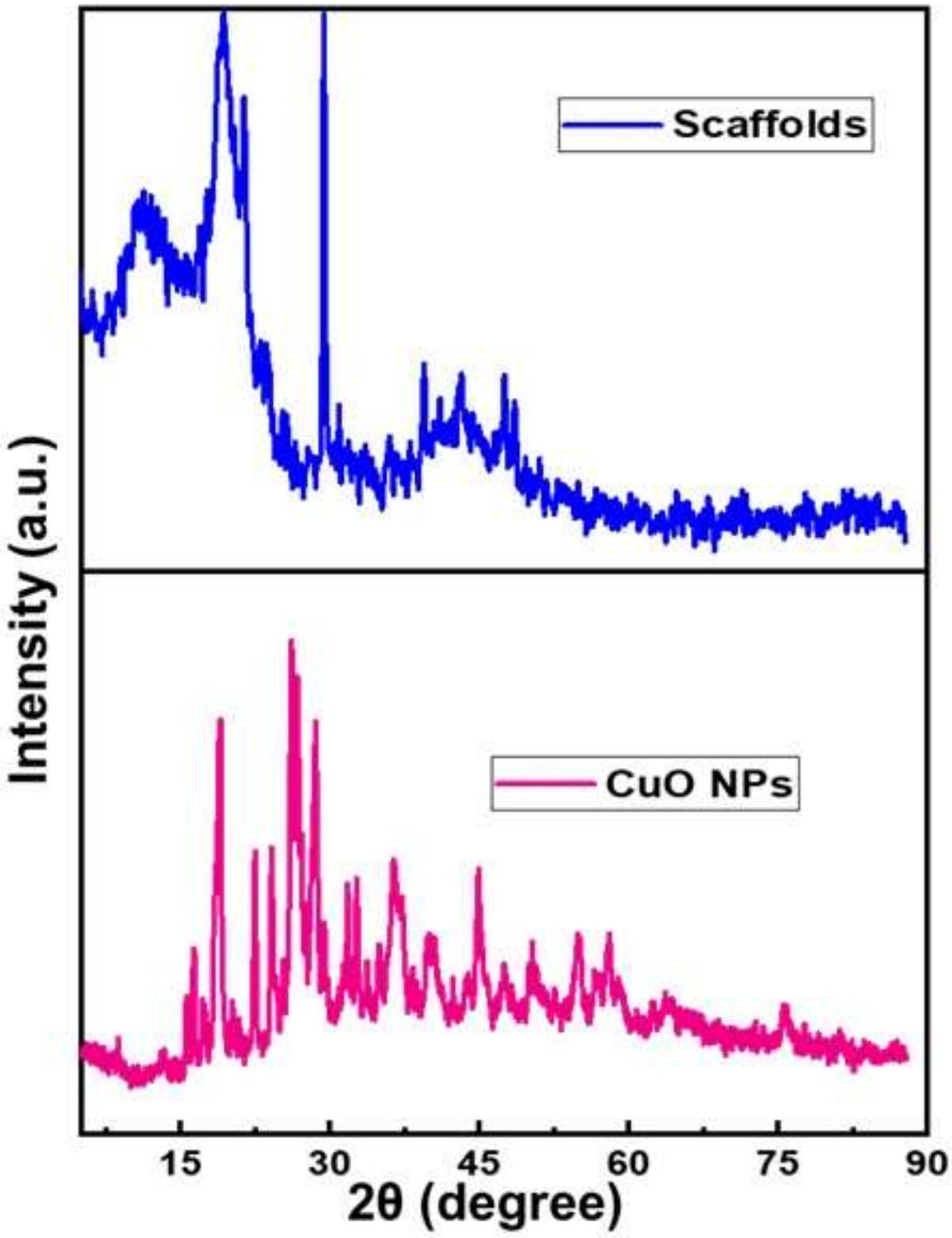

Figure 3. XRD patterns of synthesized CuO NPs and CuO-loaded scaffolds.

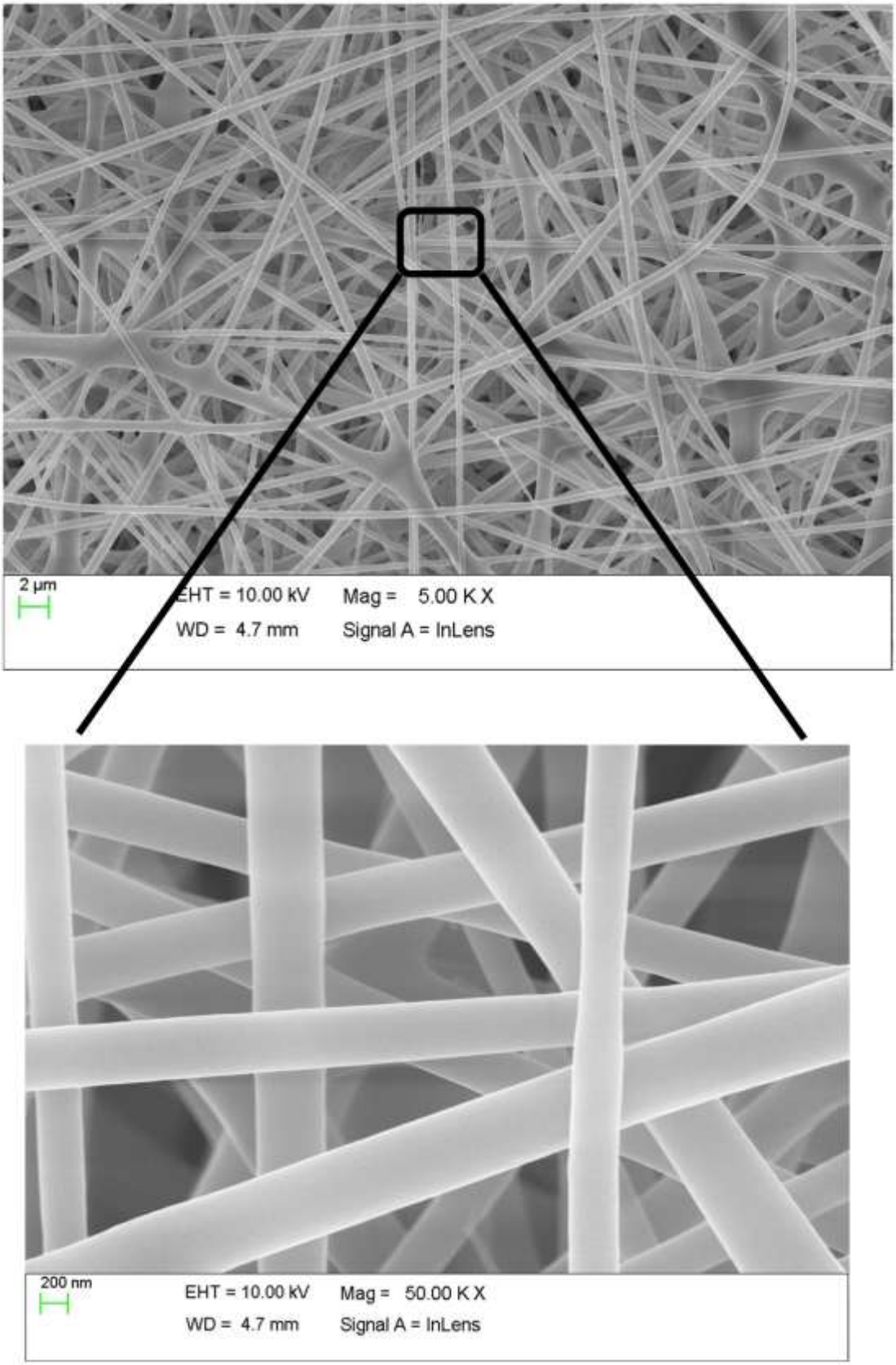

Figure4. SEM analysis of starch/PVA/CuO-NPs nanoscaffolds

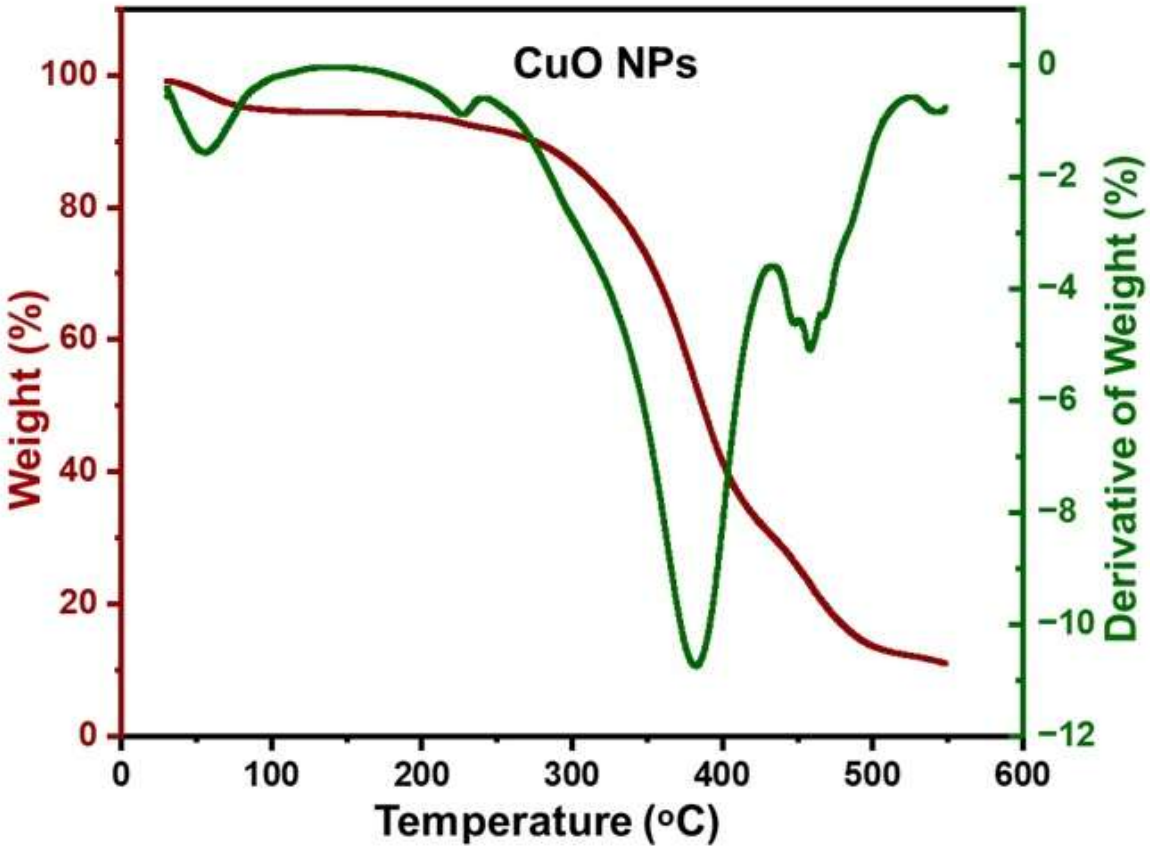

Figure 5. Thermal degradation behavior of CuO-incorporated nanoscaffolds.

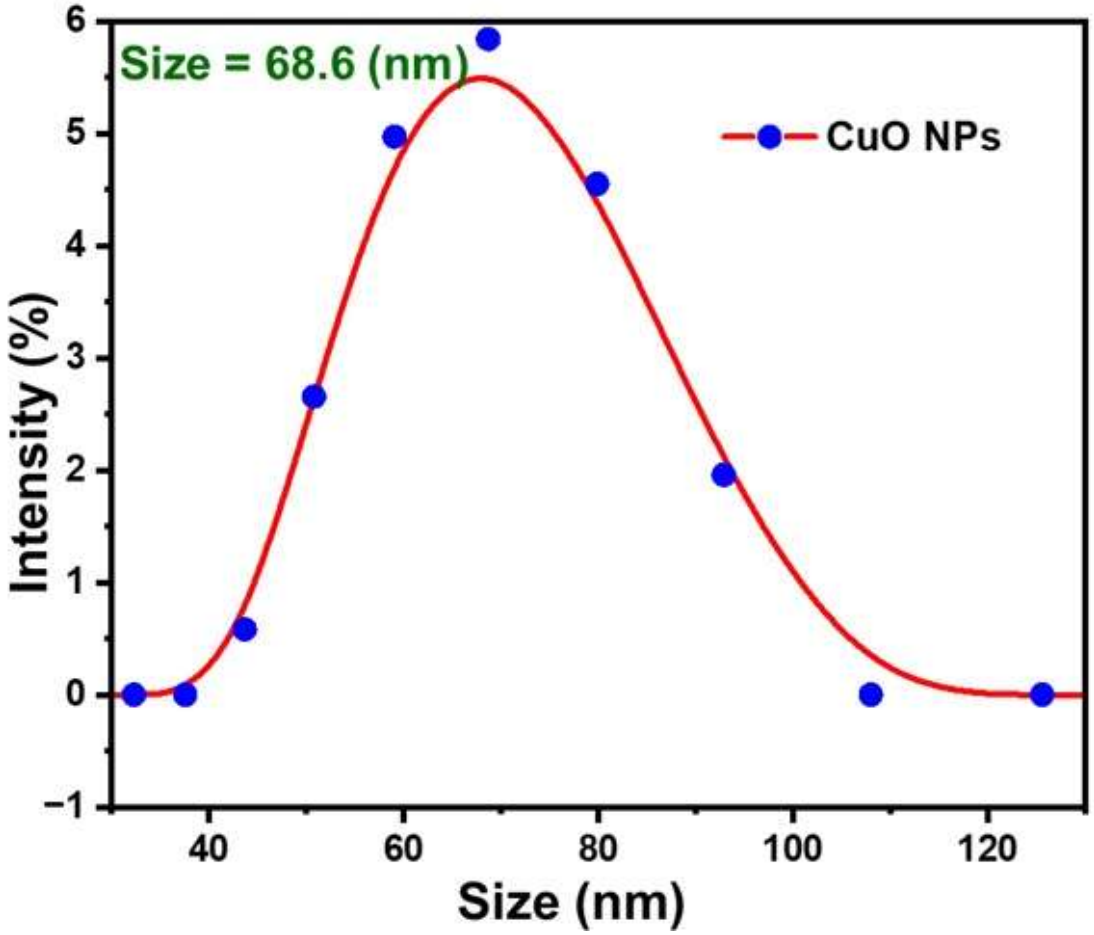

Figure6. DLS particles size analysis of CuO NPs

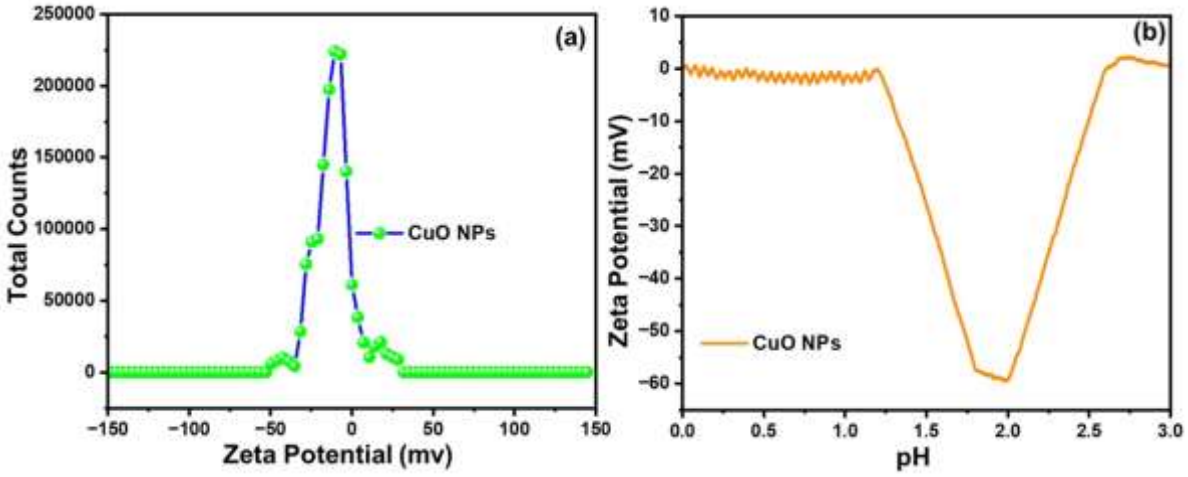

Figure7. Zeta-potential analysis of CuO NPs

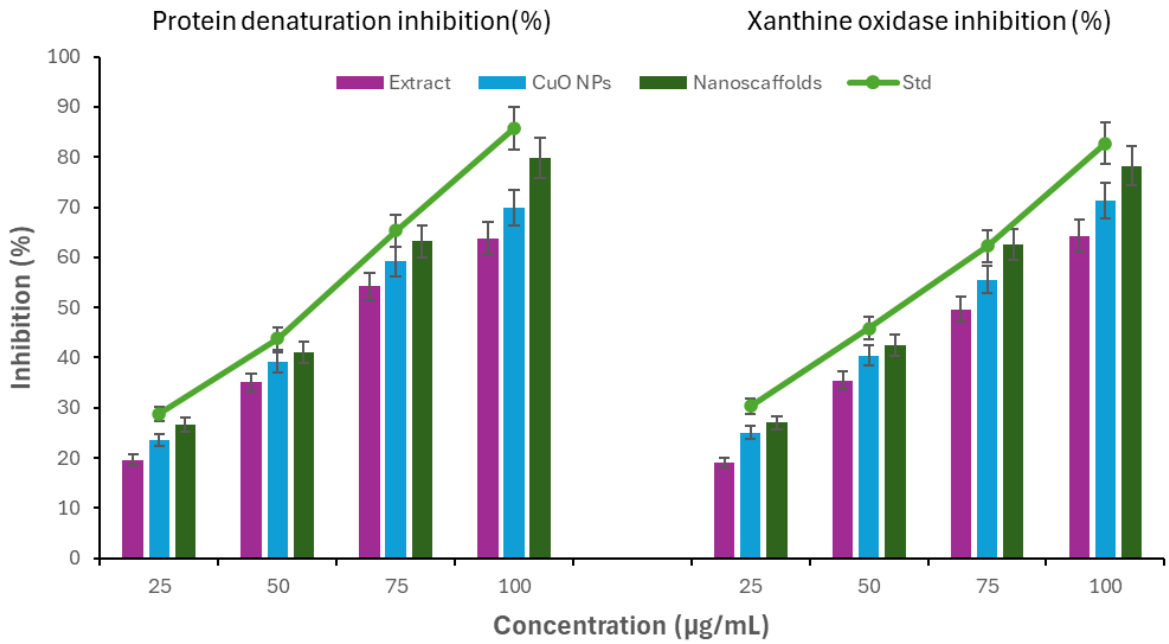

Figure8. Anti-inflammatory activity analysis of algal extract, CuO NPs and starch/PVA/CuONPs nanoscaffolds